The Cockcroft Institute
of Accelerator Science and Technology

Cockcroft-09-48

FAST, ACCURATE CALCULATION OF DYNAMICAL MAPS FROM MAGNETIC FIELD DATA USING GENERALISED GRADIENTS

D Newton and A Wolski
University of Liverpool and the Cockcroft Institute, UK

FAST, ACCURATE CALCULATION OF DYNAMICAL MAPS FROM MAGNETIC FIELD DATA USING GENERALISED GRADIENTS*

D. Newton† and A. Wolski, University of Liverpool, and the Cockcroft Institute, UK.

Abstract

Analytic descriptions of arbitrary magnetic fields can be calculated from the generalised gradients [1] of the on-axis field. Using magnetic field data, measured or computed on the surface of a cylinder, the generalised gradients can be calculated by solving Laplace's equation to find the three-dimensional multipole expansion of the field within the cylinder. After a suitable transformation, this description can be combined with a symplectic integrator allowing the transfer map to be calculated. A new tracking code is under development in C++, which makes use of a differential algebra class to calculate the transfer map. The code has been heavily optimised to give a fast, accurate calculation of the transfer map for an arbitrary field. The multipole nature of the field description gives additional insights into fringe-field and pseudo-multipole effects and allows a deeper understanding of the beam dynamics.

INTRODUCTION

Venturini and Dragt [1] give a prescription to describe a magnetic field or potential in terms of its cylindrical harmonics and Taylor expansions. Such a description gives an analytical description of the field in the transverse plane with a longitudinal dependence on the generalised gradients of the field – that is, the numerically calculated on-axis components of the field gradients. The resultant field map satisfies Maxwell's equations and automatically includes fringe field and non-linear terms. A code has been written in C++ that utilises a fast Fourier method to calculate the generalised gradients for an arbitrary magnetic field along a straight beam line. Being able to describe the fields analytically allows rapid calculation of transfer maps using a suitable analytic integration scheme. To this end, a specialised differential algebra template class is used to describe the transverse field components, and this offers significant time savings over similar, more general, codes. A second order symplectic integration scheme [2] is implemented to allow numerical or analytical computation of the evolution of the canonical phase space vector from an initial state to the final state. The modular design of the code gives a straightforward method of adding further functionality to the code, or inserting alternative components: e.g. user-defined analytical descriptions of the field, alternative integration schemes etc. As an example, an additional module has been added to describe the synchrotron radiation emitted by a particle as it traverses the field [3].

* Work supported by the Science and Technology Facilities Council, UK.

† david.newton@stfc.ac.uk

CODE DESCRIPTION

Field Description

For a periodic structure, a general scalar potential that satisfies Laplace's equation, (a cylindrical harmonic or multipole expansion) can be written:

$$\begin{aligned}\Psi &= \sum_{m=-\infty}^{\infty} \exp(\imath m\phi) \int_{-\infty}^{\infty} dk\, G_m(k)\, \exp(\imath kz) I_m(k\rho),\\ &= \sum_{m=0}^{\infty} \exp(\imath m\phi)\, \psi_m(\rho, z),\\ &= \sum_{m=0}^{\infty} \cos(m\phi)\, \psi_{m,c}(\rho, z) + \imath\, \sin(m\phi)\, \psi_{m,s}(\rho, z).\end{aligned} \tag{1}$$

$G_m(k)$ are arbitrary coefficients, and I_m are the modified Bessel functions, which can be expressed as a Taylor expansion:

$$I_m(x) = \sum_{l=0}^{\infty} \frac{1}{l!(m+l)!} \left(\frac{x}{2}\right)^{2l+m}. \tag{2}$$

From Eq. (1), the vector potentials can be derived:

$$\begin{aligned}A_\phi &= 0, \qquad (3)\\ A_\rho &= \sum_{m=1}^{\infty} \frac{\cos(m\phi)}{m} \rho \frac{\partial}{\partial z} \psi_{\omega,s} - \frac{\sin(m\phi)}{m} \rho \frac{\partial}{\partial z} \psi_{\omega,c},\\ A_z &= \sum_{m=1}^{\infty} -\frac{\cos(m\phi)}{m} \rho \frac{\partial}{\partial \rho} \psi_{\omega,s} + \frac{\sin(m\phi)}{m} \rho \frac{\partial}{\partial \rho} \psi_{\omega,c}.\end{aligned}$$

Eqs. (1) and (2) can be used to express $\psi_m(\rho, z)$ as:

$$\psi_m(\rho, z) = \sum_{l=0}^{\infty} \frac{1}{2^{2l} l!(l+|m|)!} \rho^{(2l+|m|)} \left(\frac{1}{2}\right)^{|m|} \int_{-\infty}^{\infty} dk\, k^{2l+|m|} G_m(k) \exp(\imath kz), \tag{4}$$

or

$$\psi_m(\rho, z) = \sum_{l=0}^{\infty} (-1)^l \frac{|m|!}{2^{2l} l!(l+|m|)!} \rho^{(2l+m)} C_m^{[2l]}(z), \tag{5}$$

where the $C_m^{[n]}(z)$ are the on-axis generalised gradients.

Suppose the radial component of the magnetic field, B_ρ, is known on the surface of a cylinder of radius R, then the field can be fitted in terms of a Fourier series:

$$B_\rho(\rho = R, \phi, z) = \sum_{m=0}^{\infty} \hat{a}_m(R, z) \cos(m\phi) + \hat{b}_m(R, z) \sin(m\phi) \tag{6}$$

The coefficients $\hat{b}_m$ ($\hat{a}_m$) correspond to normal (skew) components of the field, and the integer, m, gives the multipole order, i.e. $m = 0$ corresponds to a solenoid component, $m = 1$ represents the dipole component, $m = 2$ a quadrupole, etc. To calculate the generalised gradients, the Fourier series coefficients are scaled by the derivative of the Bessel function, and a Fourier transform is performed:

$$C^{[l]}_{m,s}(z) = \frac{i^l}{2^m m!} \int_{-\infty}^{\infty} dk \exp(ikz) \frac{k^{l+m-1}}{I'_m(kR)} \hat{b}_m, \quad (7)$$

and

$$C^{[l]}_{m,c}(z) = \frac{i^l}{2^m m!} \int_{-\infty}^{\infty} dk \exp(ikz) \frac{k^{l+m-1}}{I'_m(kR)} \hat{a}_m. \quad (8)$$

$C^{[l]}_{m,\alpha}(z)$ is the l th derivative with respect to z of the generalised gradients $C^{[0]}_{m,\alpha}(z)$. Eqs. (3), (5), (7) and (8) can then be used to calculate the vector potential at any point within the volume of the cylinder.

The magnetic field can be derived from the vector potentials, and transformed into Cartesian coordinates in an arbitrary gauge (see [4] for details). The field is therefore fully described in terms of its multipole modes and the generalised gradients. Furthermore, the algorithm has a smoothing quality – numerical inaccuracies in the initial field are smeared out. The modified Bessel functions, $I_m(kz)$, in Eqs. (7) and (8) mean the errors shrink exponentially as the radial distance to the axis decreases.

Differential Algebra Template Class

A "stripped-down" differential algebra template class has been written which allows polynomial expressions to be defined with an arbitrary number of variables to arbitrary order. The standard mathematical operators have been defined as well as methods for differentiation, integration, exponentiation and the trigonometric functions. Expressions, differing in the degree and number of variables (explicit instances), can be used in the same code and conversion between explicit instances is allowed. The field description is initially calculated in two variables (x, y) to order eight. Transforming to a suitable gauge (i.e. $A_x = 0$) results in a field map accurate to order six and the integration of the phase space vector therefore requires an expression in six variables to order six. The ability to mix, and convert between, classes of expressions allows a fast, efficient calculation of the final dynamical map.

Symplectic Integrator

A second order symplectic integration scheme [2] has been implemented which calculates the Lie map, $\mathcal{M}$, that transforms the canonical phase space vector $(x, p_x, y, p_y, s, \delta)$ from an initial to a final state for an integration step $\Delta\sigma$:

$$\begin{aligned}\mathcal{M}(\Delta\sigma) = &\exp\left(:-\frac{\Delta\sigma}{2}P_z:\right)\exp\left(:-\frac{\Delta\sigma}{2}a_z:\right)\\ &\exp\left(:-\frac{\Delta\sigma}{2}\left(-\delta+\frac{P_x^2}{2(1+\delta)}\right):\right)\mathcal{A}_y\\ &\exp\left(:-\Delta\sigma\frac{P_y^2}{2(1+\delta)}:\right)\mathcal{A}_y^{-1}\\ &\exp\left(:-\frac{\Delta\sigma}{2}\left(-\delta+\frac{P_x^2}{2(1+\delta)}\right):\right)\\ &\exp\left(:-\frac{\Delta\sigma}{2}a_z:\right)\exp\left(:-\frac{\Delta\sigma}{2}P_z:\right),\end{aligned} \quad (9)$$

where $a_{x,y,z}(x, y, z) = qA_{x,y,z}(x, y, z)$, and

$$\mathcal{A}_y = \exp\left(:-\int a_y(x, y, z)dy:\right).$$

This integrator was developed to allow accurate tracking through s-dependent magnetic fields (where s is the independent variable, the distance along the reference trajectory). Many magnetic elements are modelled using an impulse boundary approximation, where the magnetic field is assumed to be constant (s-independent) inside the magnet and zero elsewhere, which allows the charged particle Hamiltonian to be separated into drift and kick regions. However in many magnetic systems (e.g. wigglers and undulators) the s-dependence of the magnetic field cannot be accurately modelled in this way – the fringe fields play an important role in the charged particle dynamics. The analytical description of the field, described above, explicitly includes fringe field contributions and this symplectic integrator is well suited to describing the dynamics of a charged particle in such a field.

MODELLING THE CESR-C WIGGLER

To demonstrate the techniques mentioned above, the code was used to model the CESR-c wiggler, using simulated field data on a rectangular grid [5]. A 3D spline interpolation code was used to calculate the radial magnetic field (B_ρ) on the surface of a cylinder with a radius of 2.6 cm with 49 evenly spaced points in the azimuthal direction and 8192 points in the longitudinal (z) direction. A fast Fourier transform of this field was performed to find the coefficients $\hat{a}_m$ and $\hat{b}_m$, which were used in Eqs. (7) and (8) to calculate the generalised gradients. Fig. 1 shows the calculated normal and skew components of the generalised gradient C^0_1 (the dipole component), which corresponds to the on-axis field in the y and x directions, respectively. Because the field is calculated to some finite order (sixth, in this case) the field expansion is truncated, and the higher order components are not included. However, the number of terms can easily be increased to give greater accuracy in the final result.

Fig. 2 (left) shows the initial interpolated field map on the surface of a cylinder. Fig. 2 (right) shows the residual

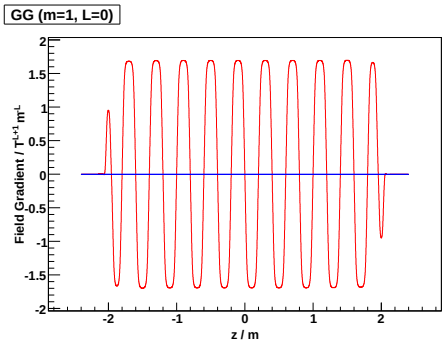

Figure 1: The C_1^0 normal (red) and skew (blue) dipole components of the generalised gradient for the CESR-c wiggler. These components are identified with the on-axis fields B_y and B_x.

difference between the interpolated field and the calculated field. The maximum difference is 2×10^{-4} T; this difference will shrink exponentially as the radial distance to the axis decreases. Outside the cylinder the uncertainties will grow exponentially, and therefore the error in the calculated field will grow rapidly.

Finally, the analytic field description was used with Eq. (9) to calculate the transfer map, and track the evolution of the dynamical variables. The energy of the electron was set to 5 GeV and 10,000 integration steps were used. At each integration step, the field components and the Lie map $\mathcal{M}$ were calculated, resulting in a transfer map for the entire magnet. The field components, calculated at each step, were written to a file, so the particle track could be quickly calculated numerically given any initial state. Fig. 3 shows the evolution of the canonical coordinates (x, p_x) over the length of the magnet for an initial state $(0, 0)$.

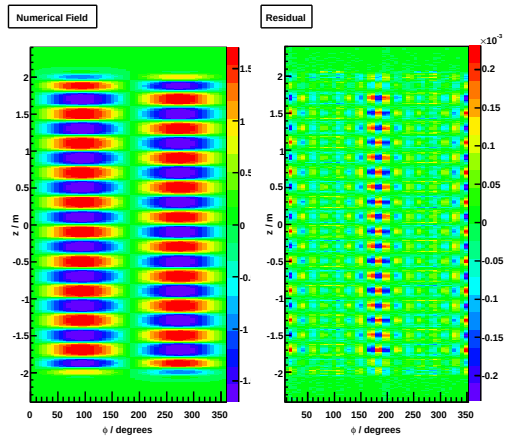

Figure 2: Left: The B_ρ component of the magnetic field on the surface of a cylinder for the CESR-c wiggler. This field is used to calculate the generalised gradients at any point within the cylinder. Right: The residual field of the input field (left) and that calculated using the generalised gradients on the surface of the cylinder.

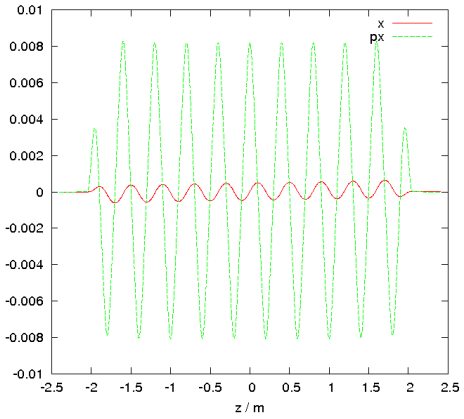

Figure 3: The evolution of the canonical coordinates (x, p_x) of a 5 GeV electron as it traverses the CESR-c wiggler. The trajectory was integrated over 10,000 points.

CONCLUSION

A new C++ code to describe arbitrary magnetic fields and calculate the evolution of the dynamical variables of a charged particle within such a field has been developed. The code is designed to provide a fast and accurate method of describing charged particle dynamics. In the given example, for a 4.8 m wiggler magnet, the field was interpolated at 49×8192=401,408 points on the surface of a cylinder. This field was used to calculate numerically the generalised gradients for the multipole components up to the 12th pole: this provides an analytical description of the transverse field. Finally, the field description was used to integrate analytically and numerically the evolution of a phase space vector (to second order in the Hamiltonian and sixth order in the field description) over the length of the magnet using 10,000 integration steps. The whole calculation took under 8 minutes with a 2.66 GHz processor. The code is modular, so additional functionality can easily be added. Further examples of the applications of this code, and an example of a module to calculate synchrotron radiation, are described in [3].

REFERENCES

[1] M. Venturini and A.J. Dragt, "Accurate computation of transfer maps from magnetic field data", Nuclear Instruments and Methods in Physics Research A, 429 (1999), 387-392.

[2] Y.Wu, E. Forest, and D.S.Robin, "Explicit higher order symplectic integrator for s-dependent magnetic field", Phys. Rev. E 68, 046502 (2003).

[3] D. Newton and A. Wolski, "Applications of a new code to compute transfer maps and describe synchrotron radiation in arbitrary magnetic fields", these proceedings.

[4] A. J. Dragt, "Lie Methods for Nonlinear Dynamics with Applications to Accelerator Physics", in preparation, Chapter 13. http://www.physics.umd.edu/dsat/dsatliemethods.html

[5] J. Crittenden, https://wiki.lepp.cornell.edu/ilc/bin/view/Public/CesrTA/WigglerInfo